J|A|C|S ARTICLES

Published on Web 10/02/2009

Simultaneous Determination of Gene Expression and Enzymatic Activity in Individual Bacterial Cells in Microdroplet Compartments

Jung-uk Shim,[†,‡] Luis F. Olguin,[†,‡] Graeme Whyte,[‡] Duncan Scott,[‡] Ann Babtie,[†] Chris Abell,[‡] Wilhelm T. S. Huck,[*,‡] and Florian Hollfelder[*,†]

Department of Biochemistry, University of Cambridge, Cambridge, CB2 1GA, United Kingdom and Department of Chemistry, University of Cambridge, Cambridge, CB2 1EW, United Kingdom

Received June 12, 2009; E-mail: wtsh2@cam.ac.uk; fh111@cam.ac.uk

Abstract: A microfluidic device capable of storing picoliter droplets containing single bacteria at constant volumes has been fabricated in PDMS. Once captured in droplets that remain static in the device, bacteria express both a red fluorescent protein (mRFP1) and the enzyme, alkaline phosphatase (AP), from a biscistronic construct. By measuring the fluorescence intensity of both the mRFP1 inside the cells and a fluorescent product formed as a result of the enzymatic activity outside the cells, gene expression and enzymatic activity can be simultaneously and continuously monitored. By collecting data from many individual cells, the distribution of activities in a cell is quantified and the difference in activity between two AP mutants is measured.

Introduction

Techniques for time-dependent measurement of the enzymatic activity of single cells are important for the analysis of populations that are to be resolved at the level of their individual members, e.g., in the study of gene expression[1,2] and phenotypic variation[3] or in the screening of protein libraries for in vivo directed evolution.[4] Fluorescence detection is frequently used to determine protein expression[1,3] or enzymatic reactions within cells, e.g., by fluorescence-activated cell sorting (FACS)[5] and microscope-based cytometry.[6,7] This method is suitable if the molecules to be detected remain in the cells or attached to them.[8] However, quantitative assessment of reaction turnover by FACS is not possible if the products of these processes leave the cells. Compartmentalizing the cells in emulsified microdroplets that retain the enzymatic reaction products overcomes this problem and allows monitoring of the enzymatic turnover of a single clone.[9,10] Encapsulation of cells in double emulsions followed by FACS has been used in studies of directed evolution,[4,11−15] thus successfully linking genotype and phenotype.[16] However, the large size variation as a result of two emulsification steps makes accurate determination of small changes in signal difficult or impossible. For a quantitative kinetic assessment of individual clones in libraries or populations, two advances are required. First, the droplet size has to be precisely controlled as the amount of product is measured optically as a concentration. Formation of droplets in microfluidic systems meets this criterion,[17,18] and several microfluidic methods have been used to isolate single cells[19−24] and quantify enzymatic activities.[2,21,25−27] Second to analyze the time-dependence in individual clones, it is necessary to immobilize the compartmentalized cells and

[†] Department of Biochemistry.
[‡] Department of Chemistry.

(1) Golding, I.; Paulsson, J.; Zawilski, S. M.; Cox, E. C. *Cell* **2005**, *123*, 1025–1036.
(2) Cai, L.; Friedman, N.; Xie, X. S. *Nature* **2006**, *440*, 358–362.
(3) Kaern, M.; Elston, T. C.; Blake, W. J.; Collins, J. J. *Nat. Rev. Genet.* **2005**, *6*, 451–464.
(4) Miller, O. J.; Bernath, K.; Agresti, J. J.; Amitai, G.; Kelly, B. T.; Mastrobattista, E.; Taly, V.; Magdassi, S.; Tawfik, D. S.; Griffiths, A. D. *Nat. Methods* **2006**, *3*, 561–570.
(5) Aharoni, A.; Thieme, K.; Chiu, C. P. C.; Buchini, S.; Lairson, L. L.; Chen, H. M.; Strynadka, N. C. J.; Wakarchuk, W. W.; Withers, S. G. *Nat. Methods* **2006**, *3*, 609–614.
(6) Gordon, A.; Colman-Lerner, A.; Chin, T. E.; Benjamin, K. R.; Yu, R. C.; Brent, R. *Nat. Methods* **2007**, *4*, 175–181.
(7) Rosenfeld, N.; Young, J. W.; Alon, U.; Swain, P. S.; Elowitz, M. B. *Science* **2005**, *307*, 1962–1965.
(8) Joensson, H. N.; Samuels, M. L.; Brouzes, E. R.; Medkova, M.; Uhlen, M.; Link, D. R.; Andersson-Svahn, H. *Angew. Chem., Int. Ed.* **2009**, *48*, 2518–2521.
(9) Griffiths, A. D.; Tawfik, D. S. *Trends Biotechnol.* **2006**, *24*, 395–402.
(10) Tawfik, D. S.; Griffiths, A. D. *Nat. Biotechnol.* **1998**, *16*, 652–656.
(11) Bernath, K.; Hai, M. T.; Mastrobattista, E.; Griffiths, A. D.; Magdassi, S.; Tawfik, D. S. *Anal. Biochem.* **2004**, *325*, 151–157.
(12) Mastrobattista, E.; Taly, V.; Chanudet, E.; Treacy, P.; Kelly, B. T.; Griffiths, A. D. *Chem. Biol.* **2005**, *12*, 1291–1300.
(13) Aharoni, A.; Amitai, G.; Bernath, K.; Magdassi, S.; Tawfik, D. S. *Chem. Biol.* **2005**, *12*, 1281–1289.
(14) Aharoni, A.; Griffiths, A. D.; Tawfik, D. S. *Curr. Opin. Chem. Biol.* **2005**, *9*, 210–216.
(15) Hai, M.; Bernath, K.; Tawfik, D.; Magdassi, S. *Langmuir* **2004**, *20*, 2081–2085.
(16) Leemhuis, H.; Stein, V.; Griffiths, A. D.; Hollfelder, F. *Curr. Opin. Struct. Biol.* **2005**, *15*, 472–478.
(17) Anna, S. L.; Bontoux, N.; Stone, H. A. *Appl. Phys. Lett.* **2003**, *82*, 364–366.
(18) Teh, S. Y.; Lin, R.; Hung, L. H.; Lee, A. P. *Lab Chip* **2008**, *8*, 198–220.
(19) Boedicker, J. Q.; Li, L.; Kline, T. R.; Ismagilov, R. F. *Lab Chip* **2008**, *8*, 1265–1272.
(20) He, M. Y.; Edgar, J. S.; Jeffries, G. D. M.; Lorenz, R. M.; Shelby, J. P.; Chiu, D. T. *Anal. Chem.* **2005**, *77*, 1539–1544.
(21) Huebner, A.; Srisa-Art, M.; Holt, D.; Abell, C.; Hollfelder, F.; Demello, A. J.; Edel, J. B. *Chem. Commun.* **2007**, 1218–1220.

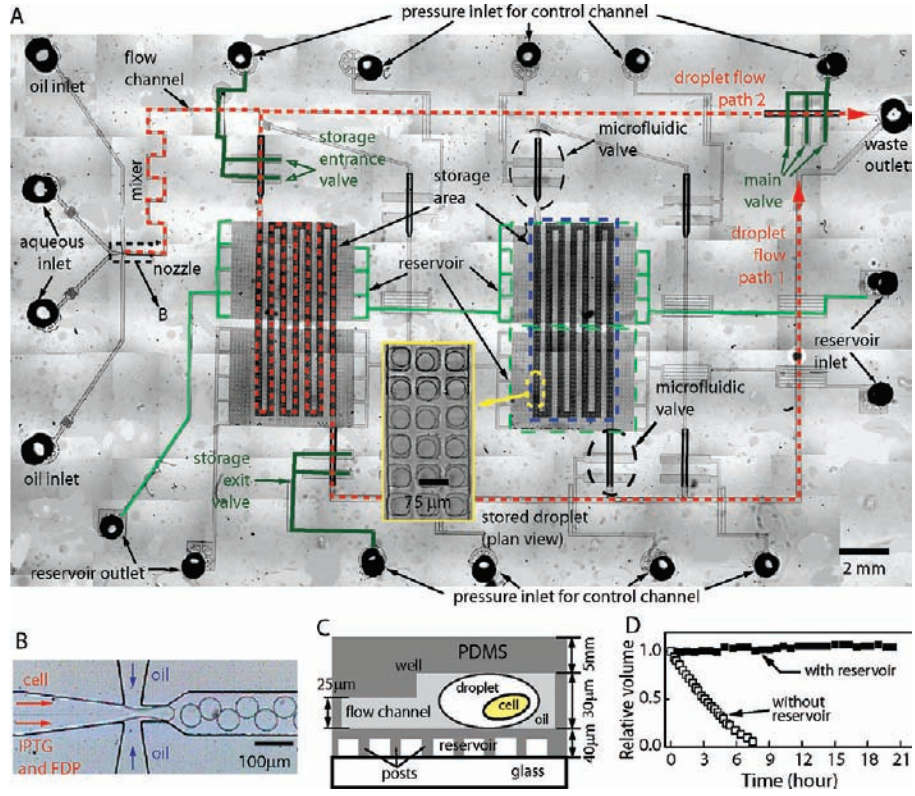

Figure 1. (A) Plan view of the microfluidic device. The orange dotted lines represent the available paths for droplets to flow from a nozzle to the waste outlet, controlled by the monolithic microfluidic valve: path-1 when the storage valve is off and the main valve is on, path 2 vice versa. (B) Droplets were formed in the flow-focusing PDMS microfluidic device. The cells and the solution containing substrate (FDP) and ITPG were combined on-chip before droplet formation. Typical droplet volume was approximately 20 pL. (C) Schematic vertical structure of the device showing an aqueous droplet stored in a well. In the upper thick (~5 mm) layer, there are flow channels and storage wells. In the lower thin (~40 μm) layer, there is a reservoir sealed by a thin PDMS membrane. (D) The change in volume of the stored droplets is less than 10% over 20 h in the microfluidic device incorporating the reservoir structure (filled squares). Water flowed through the reservoir to compensate the water evaporation from droplets into the bulk PDMS. The droplet volume shrank to less than 1/2 in 3 h in the absence of an in-built reservoir (empty squares).[33]

continuously follow reaction progress as a function of time to ensure accurate comparison between clones. FACS cannot provide the control over indexing clones and lacks the ability to accurately set the time scale for the initiation of a reaction and subsequent detection.

We have developed a microfluidic system that can simultaneously monitor the time-dependence of protein expression of monomeric red fluorescent protein (mRFP1)[28] and the enzymatic activity of coexpressed alkaline phosphatase (AP) in compartmentalized *E. coli* cells. To demonstrate the utility of this methodology for applications in directed evolution, protein expression and activity of wild type AP (WT AP) and a active mutant (R166S AP) were measured and compared.[29]

Results and Discussion

Droplet formation by flow-focusing[17,30] (Figure 1B) generated compartmentalized cells together with a substrate of the reaction and an inducer of protein expression. The components were rapidly mixed by chaotic advection by incorporating a winding channel (mixer) after the flow-focusing nozzle (Figure 1A).[31] Once formed, the droplets (~20 pL, diameter $\approx$ 30 μm) are led through flow channels controlled by monolithic valves,[32] stored into wells,[33] where they remain fixed throughout the experiment (Figure 1C). The device was built in multilayered PDMS[32,34] to incorporate microfluidic valves and wells (diameter $\approx$ 50 μm, 4000 in total) in which the droplets were arrayed to allow automated readout of the fluorescence corresponding to protein expression and product formation (Figure 1A).

(22) Clausell-Tormos, J.; Lieber, D.; Baret, J. C.; El-Harrak, A.; Miller, O. J.; Frenz, L.; Blouwolff, J.; Humphry, K. J.; Koster, S.; Duan, H.; Holtze, C.; Weitz, D. A.; Griffiths, A. D.; Merten, C. A. *Chem. Biol.* **2008**, *15*, 427–437.
(23) Baret, J. C.; Miller, O. J.; Taly, V.; Ryckelynck, M.; El-Harrak, A.; Frenz, L.; Rick, C.; Samuels, M. L.; Hutchison, J. B.; Agresti, J. J.; Link, D. R.; Weitz, D. A.; Griffiths, A. D. *Lab Chip* **2009**, *9*, 1850–1858.
(24) Edd, J. F.; Di Carlo, D.; Humphry, K. J.; Koster, S.; Irimia, D.; Weitz, D. A.; Toner, M. *Lab Chip* **2008**, *8*, 1262–1264.
(25) Schmitz, C. H. J.; Rowat, A. C.; Koster, S.; Weitz, D. A. *Lab Chip* **2009**, *9*, 44–49.
(26) Huebner, A.; Olguin, L. F.; Bratton, D.; Whyte, G.; Huck, W. T. S.; de Mello, A. J.; Edel, J. B.; Abell, C.; Hollfelder, F. *Anal. Chem.* **2008**, *80*, 3890–6.
(27) Mazutis, L.; Araghi, A. F.; Miller, O. J.; Baret, J. C.; Frenz, L.; Janoshazi, A.; Taly, V.; Miller, B. J.; Hutchison, J. B.; Link, D.; Griffiths, A. D.; Ryckelynck, M. *Anal. Chem.* **2009**, *81*, 4813–4821.
(28) Campbell, R. E.; Tour, O.; Palmer, A. E.; Steinbach, P. A.; Baird, G. S.; Zacharias, D. A.; Tsien, R. Y. *Proc. Natl. Acad. Sci. U.S.A.* **2002**, *99*, 7877–7882.
(29) Chaidaroglou, A.; Brezinski, D. J.; Middleton, S. A.; Kantrowitz, E. R. *Biochemistry* **1988**, *27*, 8338–8343.
(30) Umbanhowar, P. B.; Prasad, V.; Weitz, D. A. *Langmuir* **2000**, *16*, 347–351.
(31) Song, H.; Tice, J. D.; Ismagilov, R. F. *Angew. Chem., Int. Ed.* **2003**, *42*, 768–772.
(32) Unger, M. A.; Chou, H. P.; Thorsen, T.; Scherer, A.; Quake, S. R. *Science* **2000**, *288*, 113–116.
(33) Shim, J. U.; Cristobal, G.; Link, D. R.; Thorsen, T.; Jia, Y. W.; Piattelli, K.; Fraden, S. *J. Am. Chem. Soc.* **2007**, *129*, 8825–8835.
(34) Thorsen, T.; Maerkl, S. J.; Quake, S. R. *Science* **2002**, *298*, 580–584.

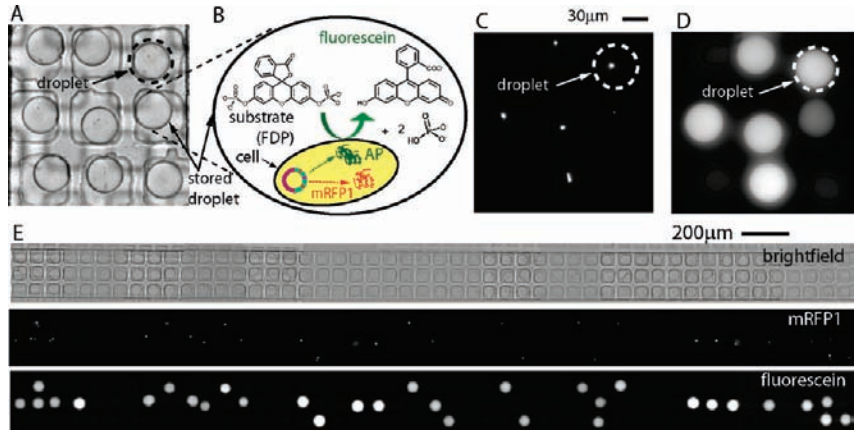

Figure 2. (A) A bright-field image of droplets stored in square wells. (B) Compartmentalized cells coexpress the two target proteins, AP and mRFP1, under the control of two identical promoters. AP hydrolyzes the substrate (FDP) to yield fluorescent products. All experiments were carried out at 30 °C. (C) Fluorescence image showing mRFP1 expression. The bright spots are cells expressing mRFP1 while encapsulated in microdroplets. (D) Fluorescence image showing the accumulation of fluorescent product uniformly distributed within the droplets. (E) Stitched micrographs showing droplets in the storage area in bright-field, red and green fluorescent images, respectively, taken 20 h after droplet formations.

Relatively wide shallow rectangular channels (typical width 100 $\times$ 30 μm) flattened the droplets in flow; however, once a droplet arrived at a deeper well, it adopted a more spherical shape, reducing its surface area and thus its surface energy. Therefore, a droplet that partially occupied both the flow channel and the well experienced a gradient in surface energy, with the resulting force acting to drive and trap the droplet inside the well as shown in Figure 1C.

Droplet shrinkage due to the water diffusion into the PDMS matrix has been previously observed in microfluidic devices.[35,36] It would jeopardize quantitative measurements of droplet contents.[37] This complication was avoided by incorporating a reservoir underneath the layer of the wells to continuously supply water to stored droplet, thereby keeping the water content of the droplets constant over longer periods (green square in Figure 1A).[33] In our experiments, we found that the evaporation rate of the droplets is balanced by the diffusion of water from the reservoir when the latter contains pure water. Figure 1D shows that in the absence of a reservoir, droplets shrank rapidly and disappeared completely in approximately 6 h. However, in the presence of a reservoir filled with water underneath the well, the droplet volume is effectively constant (within 10%) over 20 h. The ability to store droplets and maintain their volume allowed us to quantitatively monitor protein expression and enzyme activity in droplets over extended periods. The microfluidic device can be used repeatedly if cleaned appropriately after each experiment.

Cells harboring a plasmid for the coexpression of AP and mRFP1 were encapsulated in microdroplets with a fluorogenic substrate (fluorescein diphosphate, FDP) and an inducer of protein expression (isopropyl β-D-thiogalactopyranoside, IPTG) (Figure 1B). After droplet formation and deposition in the wells (Figure 2A), gene expression occurred in the presence of IPTG (Figure 2B). The fluorescence arising from mRFP1 expression remained localized in the cells (Figure 2C,E), while the fluorescent product of the alkaline phosphatase reaction spread throughout the droplets (Figures 2D,E). The mRFP1 (red emission) and fluorescein product (green emission) were simultaneously monitored over time using an EM-CCD camera coupled to an epifluorescence microscope (see Experimental Section). The system is also equipped with a motorized stage and carousel to allow accumulation of data for 4000 droplets at 20 min intervals for more than 20 h.

The time course of mRFP1 expression in individual droplets shows the onset of protein expression around 2 h after droplet formation.[7] The amount of mRFP1 increases for the next few hours before leveling out after 10 h (Figure 3A,C), possibly due to the depletion of nutrient or accumulation products of cellular metabolism.[38] The fluorescence of mRFP1 was measured from the total photon flux of all red *foci* above the droplet background. Intensities were correlated to mRFP1 concentrations by measuring a calibration curve using droplets with known mRFP1 concentrations (Supporting Information, SI, Figure S1). The time lag between droplet formation and observations of mRFP1 reflected the time required for the synthesis and maturation of the protein fluorophore.[28] The total number of mRFP1 copies lies between 0.45−2.30 million per droplet which is consistent with published data.[1]

The significant differences in expression rates of mRFP1 between droplets are primarily due to different numbers of cells in droplets as a consequence of Poissonian encapsulation of cells.[39,40] This interpretation is supported by the observation of distinct groups of droplets that provide three regularly spaced and well-defined peaks in the histogram of mRFP1 production (Figure 3B), which correspond to the initial occupancies of zero, one, or two cells per droplet. The number of droplets belonging to each peak fits the expectation of Poisson analysis (inset of Figure 3B). As an initial detection of *E. coli* in bright field images was difficult with the optical setup used, the probability of droplet population having no cell[41] ($n = 0$) was inserted into a Poisson distribution function, $f = \lambda^n \cdot e^{-\lambda}/n!$ where n describes

(35) Huebner, A.; Bratton, D.; Whyte, G.; Yang, M.; deMello, A. J.; Abell, C.; Hollfelder, F. *Lab Chip* **2009**, *9*, 692–698.
(36) Courtois, F.; Olguin, L. F.; Whyte, G.; Theberge, A. B.; Huck, W. T. S.; Hollfelder, F.; Abell, C. *Anal. Chem.* **2009**, *81*, 3008–3016.
(37) Watson, J. M.; Baron, M. G. *J. Membr. Sci.* **1996**, *110*, 47–57.
(38) Ishihama, A. *Genes Cells* **1999**, *4*, 135–143.
(39) Koster, S.; Angile, F. E.; Duan, H.; Agresti, J. J.; Wintner, A.; Schmitz, C.; Rowat, A. C.; Merten, C. A.; Pisignano, D.; Griffiths, A. D.; Weitz, D. A. *Lab Chip* **2008**, *8*, 1110–5.
(40) Chabert, M.; Viovy, J. L. *Proc. Natl. Acad. Sci. U.S.A.* **2008**, *105*, 3191–3196.
(41) Only plasmid-containing cells survive in the presence of ampicillin. This means that the lack mRFP1 signal in droplets represents no encapsulated cells.

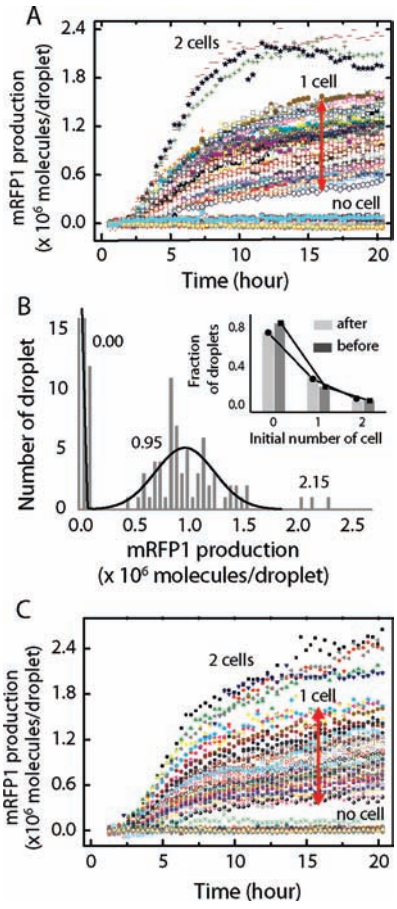

Figure 3. (A) Kinetics of mRFP1 production in cells bearing a plasmid coexpressing WT AP and mRFP1. Each time trace represents expression of mRFP1 in a different droplet. (B) Histogram showing the number of droplets plotted against mRFP1 production. The three peaks correspond to the initial number of cells encapsulated per droplet. A total of 239 droplets were analyzed: 64 droplets contained initially one cell, 3 droplets two cells, and 172 droplets were empty. Gaussian envelopes for the first and second peak were drawn to guide the eye. The values presented next to each peak are averages of mRFP1 production in each group of droplets. The inset represents the fraction of droplets and the initial number of cells therein, based on mRFP1 fluorescence (light gray: expression after encapsulation, dark gray: control experiment with mRFP1 expression before encapsulation). The populations observed coincide exactly with the values predicted by the Poisson analysis (black circles and squares). (C) Time course of mRFP1 production in cells bearing a plasmid coexpressing R166S AP and mRFP1. These can be clustered into three groups as was done for the coexpression of WT AP and mRFP1.

the initial number of cells in a droplet, then the average cell number (λ) was obtained. It gives a whole distribution (f) of droplet population as a function of the initial number of cells. In addition, the distribution of droplet populations with different numbers of cells derived in a control experiment, in which cells had expressed mRFP1 before encapsulation and thus were immediately detectable, was shown to follow a similar Poisson distribution (inset of Figure 3B).

There is significant intra group variation (0.45−1.55 millions copies of mRFP1 per droplet) in the group that started with one cell (Figure 3B). Several explanations for this observation can be advanced,[42] including variations in the copy number of plasmid DNA and differences in expression levels among a population of cells. In addition, compartmentalized cells were dividing on the time scale of the experiment, so differences in individual cell growth and division rates could also contribute to the observed divergence. This is supported by the observation of cell occupancies of 3−7 cells per droplet after 20 h.

The time courses for fluorescein formation in droplets are shown in Figure 4A. The fluorescein concentration started to increase approximately 4 h after droplet formations, i.e., 2 h after the onset of mRFP1 formation. This may reflect the necessity of periplasmic export for AP, where it meets the negatively charged substrate that cannot readily enter the cytoplasm.[43] The fluorescein production rate rapidly increased after 4 h and was maintained for next the 5−7 h, falling again after around 10 h, which is presumably due to the inhibition of enzyme activity by the accumulation of phosphate products or product leaking out of the droplets.[36] The enzymatic rates observed in individual droplets fall into three distinct groups as observed for mRFP1 expression, again reflecting the number of cells initially compartmentalized (Figure 4B). The average production rate of droplets assigned as containing two cells (3.69 μM/hour) is twice that of the group containing one cell (1.83 μM/hour).

The microfluidic platform was used to differentiate the activities of WT AP from its mutant R166S AP. The maximum average production rate of fluorescein is 1.83 μM/hour at 8.6 h for WT AP and 1.04 μM/h after 10.3 h for R166S AP. The differences in the time lag and the production rate are due to the lower activity of the mutant. The activities of purified WT and R166S AP (k_{cat}/K_M) differ by up to 300-fold,[29,44] but the product formation is limited by substrate diffusion into the periplasm[43,45] and differing inhibition by phosphate[44] leading to smaller observed differences in cell-based assays. Figure 4D shows an enzymatic whole-cell activity assay in a microtiter plate that matches the average value measured in microdroplets, although it sums up the activities of millions of individual cells. Interestingly, the droplet-based experiments on the WT AP and the R166S mutant show significant differences in heterogeneity of individual compartmentalized cells. The fluorescein production shows a 3−7 h spread in lag times for the R166S mutant, whereas the WT AP fluorescein production is more narrowly distributed (Figure 4A,C). Simultaneous measurements of the fluorescence intensity of both mRFP1 and the product of enzyme reaction in droplets allows normalization of enzymatic activities using mRFP1 as an internal standard.

The variation between cells in protein expression level may make it difficult to distinguish two mutants simply by monitoring fluorescein production. Normalizing the fluorescein production rates to the mRFP1 expression rate observed in any particular droplet enables a correction that allows access to the specific enzyme activity. This normalization removes the variance introduced by different copy numbers of plasmid DNA, different global expression levels or different numbers of cells in droplets. However, the distribution of droplet populations after normalization still shows variations, which can be described by a Gaussian fit (Figure 5A). These variations can be ascribed to fluctuations of the relative expression level of AP and mRFP1 despite both being expressed from the same plasmid. Mutant and wild-type enzyme can be distinguished, but there is a considerable overlap (~50% of the respective populations).[46]

(42) Avery, S. V. *Nat. Rev. Microbiol.* **2006**, *4*, 577–587.
(43) Martinez, M. B.; Schendel, F. J.; Flickinger, M. C.; Nelsestuen, G. L. *Biochemistry* **1992**, *31*, 11500–11509.
(44) O'Brien, P. J.; Herschlag, D. *Biochemistry* **2001**, *40*, 5691–5699.
(45) Martinez, M. B.; Flickinger, M. C.; Nelsestuen, G. L. *Biochemistry* **1996**, *35*, 1179–1186.

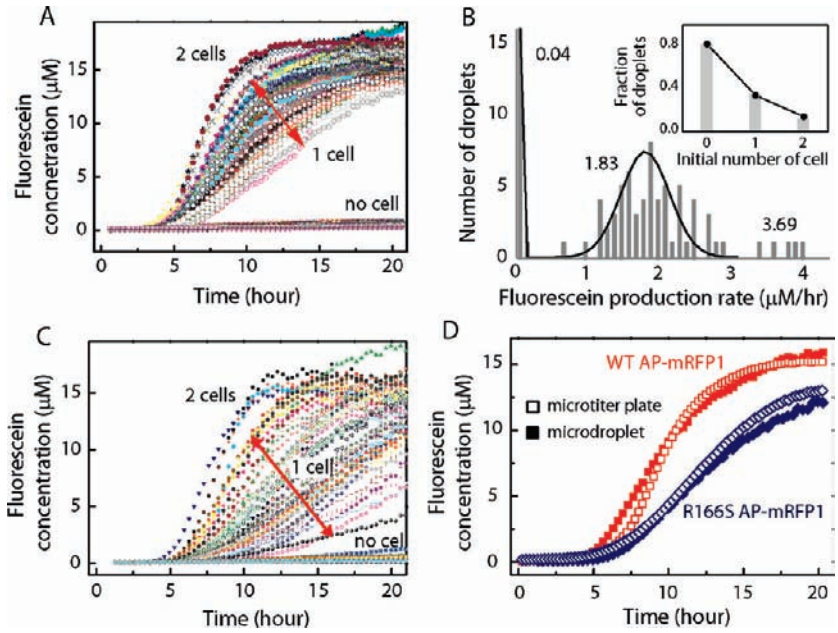

Figure 4. (A) Fluorescein concentration due to enzymatic activities of WT AP coexpressed with mRFP1 over time. Each series of symbols represents product formation in individual droplets starting with no cell (background hydrolysis), one or two cells. (B) The number of droplets was plotted against the fluorescein production rate of WT AP. Gaussian envelopes for the first and second peak were drawn to guide the eye. The values presented next to each peak are averages of the fluorescein production rate in each group of droplets. The inset represents the population of droplets against the initial number of cells therein. The bars in light gray are the fraction of droplets belonging to the each peak in the histogram. The circular spots represent fractions predicted by the Poisson distribution based on the same number of empty droplets. (C) Fluorescein concentration arising from enzymatic turnover of R166S AP, coexpressed with mRFP1 over time. (D) The comparison of the time courses of fluorescein production of WT AP and R166S, both coexpressing mRFP1, measured in the microfluidic system and compared to an analogous experiment in a conventional microtiter plate reader.

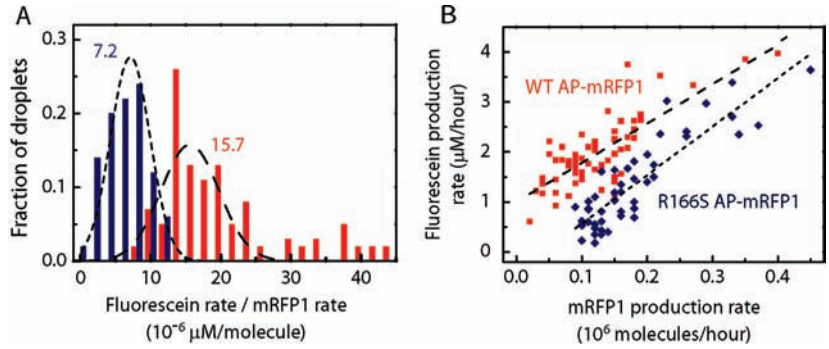

Figure 5. (A) Histograms displaying the number of droplets against fluorescein production rate normalized by mRFP1 expression rate. These rates were obtained as the steepest slopes in time courses of product formation or mRFP1 expression in each droplet. The bars in red and blue are distributions of droplets containing cells harboring plasmids producing wild-type and R166S AP, respectively, while coexpressing mRFP1. The values displayed next to each Gaussian are averages of the rate ratios. Data from 67 or 50 droplets (for WT and R166S, respectively) were analyzed for the histograms. (B) The fluorescein production rate was plotted against the mRFP1 expression rate. Wild-type AP (squares in red) produces more product than R166S AP (diamonds in blue). Lines on each set of symbols are drawn with the linear least-squares fit.

By constructing a plot correlating mRFP1 and fluorescein production rate (Figure 5B), populations of WT and R166S AP become more clearly distinguishable. The linearity of each series implies that mRFP1 expression is correlated with fluorescein production and hence AP expression.[47]

The distribution of droplets expressing R166S AP (blue bars in Figure 5A) is shifted to a lower fluorescein production rate consistent with lower activity in cell-based assays, despite similar expression levels measured by mRFP1 production (Figure 3A,C). The wild-type AP expressed in cells produced fluorescein ~2× faster than R166S AP for a given amount of mRFP1. A number of salient features in Figure 5A distinguish WT and mutant. The width of the curve for the R166S AP is smaller than for the WT AP.[48] In the case of the WT AP (red bars), ~16% of cells are outliers that do not follow the normal distribution and exceed the most populated activity of wild-type, i.e., more fluorescein was produced than would be expected, spanning a concentration range between 30−45 μM of fluorescein per million molecules of mRFP1. As mRFP1

(46) The two-tail p-value for the null hypothesis that these two distributions have the same mean is $\ll$0.01. Therefore, the difference observed between the WT and mutant populations is statistically relevant.

(47) Fusions of the protein of interest with fluorescent reporter proteins can be used to relate protein concentration and catalytic activity (see ref 52). However, a purified fusion protein of AP and mRFP1 is 10-fold less active in k_{cat}/K_M compared to WT AP, and export and expression levels of the fusion protein may differ in cell-based assays, where it appears less active (SI Figure S2).

(48) The standard deviation of the curves are 2.9 and 4.1 (μM per million molecules of mRFP1) for R166S and WT, respectively.

coexpressed with WT AP and R166S AP are produced at similar levels, these outliers are presumed to derive from clones in which the regulation of protein production from the pDuet vector was biased toward the second reading frame, and the variance represents imbalances between AP and mRFP1 expression that limits the normalization.

Experimental Section

Device Fabrication. The microfluidic circuit was designed with AutoCad (AutoDesk) and high resolution photo masks were fabricated on transparencies (Circuit Graphics, Essex, UK). Negative photoresist (SU8−2025, SU8−2007 Microchem Inc.,) was used to fabricate the flow channel, wells and valve-reservoir channel, and positive photoresist (AZ-9260, AZ Electronic Material) was employed to build the valve channel which performed better with a rounded shape.[49]

A commercially available liquid PDMS kit (Sylgard184, Dow Corning) containing the prepolymer and a cross-linker, was used in the recommended weight ratio of 10:1. The microfluidic device was made out of two masters. The first master contained the flow channel, the valve channel and the well channel. The second master contained the control channel and the reservoir. The weight ratio for a thick (5 mm) PDMS slab was 5:1 and 20:1 for the thin PDMS layer (∼40 μm). Thus, each layer had an excess of one of the components. The mixed, degassed liquid PDMS (at a 5:1 ratio) was poured onto the first master and cured at 75 °C for 25 min. The resulting transparent, flexible silicone rubber was peeled off, leaving relief features from the master imprinted onto the PDMS slab. Injection holes were punched through the slab to insert tubes that carried the fluid inlets. In order to fabricate the control channel and the reservoir in the device, a thin PDMS layer was added onto the face of the PDMS slab before covering it with a glass substrate. The thin layer was formed by spinning at a 20:1 ratio of liquid PDMS on the second master. The wafer was cured at 85 °C for 5 min. When assembling the thick PDMS slab onto the thin PDMS layer, precise optical alignment was required to put the valve channel above the control channel, and ensure the positioning of the reservoir underneath the well.

The device was then baked again at 85 °C for 30 min to enhance adhesion between two PDMS layers. While baking, the excess of cross-linker diffused from the thick layer into the thin layer.[32] Further curing caused the two layers to form cross-linked elastomer at the interface. Injection holes were punched with the lure stub adapters to insert tubing. The device was sealed against a glass substrate after plasma oxidation.[50] Finally, CYTOP (Asahi glass company) was applied to coat the flow channels to prevent water from sticking to the PDMS device.[33]

Device Operation. Aqueous droplets were formed in fluorinated oil (FC-40, 3M) at the nozzle of the device. The oil was mixed with surfactants and 16% w/w tridecafluoro octanol (Sigma-Aldrich) to prevent the coalescence of droplets.[51] The reservoir constructed underneath the wells supplied water to droplets through the PDMS membrane via an osmotic pressure gradient,[33] maintaining the volume of stored droplets. Water flowed through the reservoir during the droplet incubation period when gene expression in cells was induced at 30 °C. The volume of the stored droplets changed by less than 10% of their initial volume during the reaction time of 20 h (Figure 1D).

Cell Preparation. A single colony of *E. coli* BL21(DE3) freshly transformed with the plasmid for coexpression of mRFP1 and alkaline phosphatase was used to inoculate 2.0 mL of tryptone broth (10.0 g Peptone from casein (Merck) and 5.0 g NaCl/L)[43] containing kanamycin (30 μg/mL). The culture was grown for 2 h at 37 °C. Then, 1.0 mL of the cell culture was filtered (Minisart 5 μm, Sartorius) and diluted to a final A^{600} of 0.04 with tryptone broth containing kanamycin (30 μg/mL) and 25% Percoll (v/v, Sigma-Aldrich). This mixture was loaded in a syringe (Gastight, Hamilton) and injected into the microfluidic device. Before droplet formation, this cell suspension was mixed prior to entering a flow focusing geometry (Figure 1B) in a 1:1 ratio with Solution A (tryptone broth supplemented with 200 mM MOPS buffer pH 7.6; 30 μg/mL of kanamycin; 0.5 mM IPTG and 100 μM of fluorescein diphosphate). As a control experiment, 100 μL of the cell suspension was combined with 100 μL of Solution A. This mixture was incubated at 30 °C in a sealed 96-well plate for 20 h, and the changes in fluorescence at 530 nm were recorded (Figure 4D).

Data Acquisition and Analysis. The fluorescence images were obtained using an inverted microscope (IX71, Olympus) operated in epifluorescence mode using a mercury lamp (U-LH100HG, Olympus) for wide-field illumination. The sample was illuminated and the image collected using the same objective (UPLSAPO 40 × 2, Olympus). The fluorescence emission was separated from the illumination using fluorescence mirror sets (U-MF2, U-MWIG3, Olympus). The two colors of fluorescence were acquired sequentially using an automated mirror changer (IX2-RFACA-1−5, Olympus). To image large areas of the device, the device was mounted to a motorized stage (H117 ProScan II, Prior Scientific) that moved the device in a predefined pattern. The sample was only illuminated during the acquisition, by means of a computer-controlled shutter in the illumination arm (SmartShutter, Sutter Inc.) to minimize photobleaching. The emission image was acquired using an EM-CCD camera (Xion+, Andor Technologies) and saved to the computer hard disk for offline analysis. Time course measurements were performed using bespoke software written in LabView (National Instruments). Image analysis was performed using Bespoke software written in LabView. To measure the concentration of fluorescein, regions of interest were defined within the droplet, and the mean intensity was calculated. The fluorescence intensity of mRFP1 was calculated as the integral of the measured fluorescence across the entire droplet, after background subtraction.

Conclusions

By using the microfluidic system described in this work, it was possible to maintain thousands of droplets in a constant environment that allows quantitative measurements of each droplet and enabled the concurrent study of the kinetics of protein expression and enzymatic activity in individual cells. The ability to simultaneously monitor these properties provides an analytical tool for the assessment of members of a library in a directed evolution experiment or allows interrogation of the heterogeneity of cells generated from an identically prepared ensemble.

Acknowledgment. This research was supported by a RCUK Basic Technology Grant, the EU NEST MiFem and the EPSRC. We thank D. Bratton and A. Theberge for surfactant synthesis, and R.Y. Tsien for the mRFP1 gene. J.U.S. thanks the EU for a Marie-Curie fellowship, A.B. thanks the BBSRC and Glaxo Smith Kline for a CASE studentship. F.H. is an ERC Starting Investigator.

Supporting Information Available: DNA constructs, surfactant synthesis and further kinetic data. This material is available free of charge via the Internet at http://pubs.acs.org.

JA904823Z

(49) Studer, V.; Hang, G.; Pandolfi, A.; Ortiz, M.; Anderson, W. F.; Quake, S. R. *J. App. Phys.* **2004**, *95*, 393–398.
(50) Duffy, D. C.; McDonald, J. C.; Schueller, O. J. A.; Whitesides, G. M. *Anal. Chem.* **1998**, *70*, 4974–4984.
(51) Holtze, C.; Rowat, A. C.; Agresti, J. J.; Hutchison, J. B.; Angile, F. E.; Schmitz, C. H. J.; Koster, S.; Duan, H.; Humphry, K. J.; Scanga, R. A.; Johnson, J. S.; Pisignano, D.; Weitz, D. A. *Lab Chip* **2008**, *8*, 1632–1639.
(52) Gupta, R. D.; Tawfik, D. S. *Nat. Methods* **2008**, *5*, 939–942.